

# 1 Towards Sarcosine Determination in Urine for Prostatic Carcinoma Detection

2

3 Neus Jornet-Martínez<sup>1,2</sup>, Cassi J Henderson<sup>1,3</sup>, Pilar Campíns-Falcó<sup>2</sup>, Ronan Daly<sup>3</sup> and  
4 Elizabeth A H Hall<sup>1\*</sup>

5

6 *1. Department of Chemical Engineering and Biotechnology, University of Cambridge, Philippa Fawcett  
7 Drive, Cambridge, CB3 0AS, UK.*

8 *2. MINTOTA Research Group, Department of Analytical Chemistry, Facultat of Chemistry, University of  
9 Valencia, C/ Doctor Moliner, 50, Burjassot, 46100, Valencia, Spain*

10 *3. Institute for Manufacturing, University of Cambridge, Charles Babbage Road, Cambridge, CB3 0FS,  
11 UK*

12

## 13 **Abstract.**

14

15 Sarcosine, a potential biomarker for prostate cancer, can be detected in a solid state enzyme  
16 based biosensor using sarcosine oxidase, with particle immobilised reagents. A novel fusion  
17 protein of the fluorescent protein, mCherry, sarcosine oxidase (SOx), and the polypeptide R5  
18 (R5<sub>2</sub>-mCherry-SOx-R5-6H), was explored, which allowed self-immobilization on silica  
19 microparticles and long-term (90 days +) retention of activity, even at room temperature. In  
20 contrast, commercial wildtype SOx lost activity in a few days. A silica-R5<sub>2</sub>-mCherry-SOx-R5-  
21 6H microparticle sensor for determination of sarcosine in urine, linked the SOx coproduct,  
22 H<sub>2</sub>O<sub>2</sub>, to a measurement catalysed by horseradish peroxidase (HRP) immobilised on silica, in  
23 the presence of Amplex Ultrared (AR) to generate fluorescence at 582 nm. Silica microparticles  
24 carrying all the reagents (R5<sub>2</sub>-mCherry-SOx-R5-6H, HRP and AR) were used to produce a  
25 silica-microparticle biosensor which responded to sarcosine at micromolar levels. Interference  
26 by amino acids and uric acid was examined and it was found that the silica-reagent carrying  
27 system could be calibrated in urine and responded across the clinically relevant concentration  
28 range. This contrasted with similar assays using commercial SOx, where interference inhibited  
29 the sarcosine signal measurement in urine. The microparticle biosensor was tested in urine from  
30 healthy volunteers and prostate cancer patients, showing higher concentrations of sarcosine in  
31 cancer patients consistent with previous reports of elevated sarcosine levels.

32

33 **Keywords** Silaffins, Enzyme immobilization, Biosensor, Sarcosine, Prostatic carcinoma, urine

34

## 35 **1. Introduction**

36

37 Development of in vitro diagnostics (IVDs) to guide earlier diagnosis and more effective

38 clinical intervention with improved cost effectiveness has become a clear objective in sensor  
39 research [1]. Cancer is not yet well represented in IVD diagnostics, but the need for early  
40 detection and triage is undisputed. It has been noted by Soper et al. [2] that point of care  
41 diagnostics for cancer have been slow to evolve for a variety of reasons. In some cancers this is  
42 partly due to the lack of known robust biomarkers that could act as targets in a diagnostic. In  
43 other cancers, some progress could be made with the production of the right reagents for  
44 identified biomarkers.

45

46 Prostate cancer, for example, is one of the leading causes of cancer death among men [3].  
47 Although widely used in connection with cancer, detection of elevated levels of prostate-  
48 specific antigen (PSA) will identify prostate disease, but not necessarily prostate cancer. When  
49 the test was first introduced in 1986, it was intended as a marker of disease progression, in  
50 already diagnosed patients, not for cancer diagnosis, but its wider use [4] and the resulting  
51 ambiguity in the result is now driving the search for better biomarkers and thence IVDs [5-7].  
52 Thus, biopsy and digital rectal examination (DRE) are still the best first approach [8] in  
53 combination with PSA testing. Centralised laboratory testing further supports diagnosis with,  
54 for example, transrectal ultrasound [9] guiding biopsies [10] and an increasing use of magnetic  
55 resonance [11] and positron emission tomography [12].

56

57 PSA is typically measured in blood or serum (recently a study in saliva has also been reported  
58 [13]), but *to add value* to the PSA test, urine based biomarkers are of special interest, that can  
59 be ‘co-detected’ without invasive sampling, as described by Cao et al [7]. Molecular biomarkers  
60 (metabolite, gene and protein based) are being identified that collectively may lead to better  
61 diagnostics [14, 15] and, in this context, the amino acid, sarcosine (N-methylglycine) has been  
62 studied in both blood and in urine as a marker of early-stage prostate cancer [16]. Although the  
63 measurements in blood have been reported as unremarkable, significantly elevated levels in  
64 urine have been recorded in some studies, for patients with prostate cancer. Furthermore, in a  
65 recent study cancer sniffer dogs were able to distinguish artificial urine samples that had been  
66 doped with sarcosine, with 90% success rate [17]. The possible role of sarcosine is however still  
67 strongly debated [18], but some recent studies have suggested that sarcosine exhibits  
68 considerable stimulatory effects on growth in malignant/metastatic prostate cells [19], possibly  
69 due to accumulation in the tumor and consequential conversion to serine and glycine, thereby  
70 providing tumor growth promoters [20,21].

71 Laboratory based techniques for sarcosine detection are typically high performance  
72 chromatography [22], whereas several different approaches have been suggested to provide a  
73 nearer-patient diagnostic. For example, Biavardi et al., [23] designed a direct binding cavitand,

74 anchored on a Si-substrate, that showed a change in the fluorescence in the presence of  
75 sarcosine, whereas Valenti et al., [24] used the same cavitand to provide selectivity in an  
76 electrochemiluminescence system. In contrast, others have proposed an immunoassay [25] which  
77 was able to discriminate sarcosine in urine samples with good sensitivity and without undesired  
78 interference in well controlled assay conditions, although quantification in a near-patient  
79 diagnostic measurement remains challenging.

80

81 Currently available sarcosine test *kits* mainly use a classical oxidase linked assay, and although  
82 there are reports of amperometric sarcosine biosensors with sarcosine oxidase, using the same  
83 principle as first and second generation glucose oxidase biosensors [26], most of the test kits  
84 that are already available are colorimetric or fluorometric versions of this classical oxidase assay.  
85 These are based on an indirect measurement of sarcosine via the coproduct H<sub>2</sub>O<sub>2</sub>, catalysed by  
86 horseradish peroxidase and taking advantage of the myriad of dyes that can be coupled into this  
87 reaction as indicator. Nevertheless, although these types of kit are suitable for use in plasma and  
88 serum, interference in measurements made in urine is typically reported, producing erroneous  
89 results. Some attention has been given to overcoming this interference, for example Lan et al.  
90 used 3,3',5,5'-tetramethylbenzidine with palladium nanoparticles as a catalyst instead of  
91 horseradish peroxidase [27] and Burton et al. directed their attention to the other coproduct  
92 (formaldehyde) and the pH change associated with its conversion to formic acid under  
93 optimised conditions [28]. However, these methods have required quite a lot of laboratory based  
94 processing in the analytical pathway; for example the latter method [28] requires the introduction  
95 of NaOH and heat, for the Cannizzaro reaction to proceed which converts the formaldehyde to formic  
96 acid and methanol and degrades the hydrogen peroxide. This isn't suitable for development of a  
97 biosensor and thus, interference of the measurement in urine remains a challenge for a near  
98 patient diagnostic.

99

100 Most of these assays use solution based reagents. However, it has been reported that  
101 immobilized enzymes can in some cases, exhibit higher selectivity and sensitivity [29], but on  
102 the other hand, chemical modification during immobilization can cause enzyme degradation or  
103 block the active centre, or result in the enzyme orientation being incorrect for reaction with the  
104 enzyme substrate. [30] Peptide molecular biology immobilization techniques can be inspired by  
105 high affinity peptides from binding patterns in nature [31] which allows an immobilisation  
106 functionality to be fused with the reagent enzyme (e.g. sarcosine oxidase) during protein  
107 expression. This allows attachment of the protein on a surface to be in-built without further  
108 chemical modification and may help to better retain enzyme activity. We have recently taken  
109 inspiration from "Garage Biotech" [32] and shown that an engineered sarcosine oxidase (SOx),  
110 immobilised on silica via a silaffin peptide tag [33] can retain exquisite selectivity for sarcosine.

111 A simple one-step isolation-to-use method is presented which produces a silica particle-enzyme  
112 sensor. It is low cost, biocompatible and stable in most biosystems [34].

113

114 We have therefore returned to the sarcosine oxidase linked assay and considered whether the  
115 assay can be optimised for measurement in urine by focusing on the presentation of the enzyme  
116 and other reagents, and thereby, develop a biosensor where all the reagents are immobilized on  
117 a solid support, leading to good point of care usability, rapid result outcome. Successful  
118 (bio)molecule immobilization has been demonstrated to be beneficial for diverse  
119 biotechnological and medicinal applications [35]. In the research reported herein, we use both  
120 chemical immobilisation techniques and protein engineering to improve long term protein  
121 stability and aid performance in the design of in vitro diagnostics (IVD). We used the novel  
122 enzyme-silica combination in order to study its compatibility in urine and to develop a  
123 fluorometric sensor for sarcosine detection in human urine, by incorporating all needed reagents  
124 in silica. A first small sample test shows discrimination between healthy and prostate cancer  
125 volunteers.

126

127

## 128 **2. Materials and methods**

129

### 130 2.1 Materials and reagents

131

132 Enzymes used for cloning (restriction enzymes, calf intestinal alkaline phosphatase, Antarctic  
133 phosphatase, T4 DNA ligase) and Quick Ligation kit were purchased from New England  
134 Biolabs and were used according to the manufacturer's instructions. Plasmid pET24a (Novagen)  
135 containing the R5<sub>2</sub>-mCherry-mSOx-R5-6H gene was produced previously in the Hall  
136 laboratory, Cambridge. Details have been reported previously [33].

137

138 The enzyme sarcosine oxidase from *Bacillus* sp. (25-50 units/mg), peroxidase from horseradish  
139 (50-150 units/mg), lysozyme from chicken egg white lyophilized powder and the analyte  
140 sarcosine were purchased from Sigma Aldrich (Saint Louis, USA). The particles used were  
141 glass bubbles microspheres/microballoons from easycomposites (Stoke-on-Trent, UK), gel  
142 silica particles <63 µm from Fluka (Monte Carlo, Monaco), TLC-Kieselgel 60H average  
143 particle size 15 µm (90% between 3.5 – 25µm) from Merck (Darmstadt, Germany) and  
144 microparticles from YMC (Hong Kong, China) (range 63-210µm) and glass beads unwashed  
145 (450-600 µm) were from Sigma Aldrich (Saint Louis, USA). The silica particles were modified  
146 with tetraethyl orthosilicate, 3-(aminopropyl)triethoxysilane ammonium hydroxide solution (28-  
147 30%) from Sigma Aldrich (Saint Louis, USA). The fluorescent probe Amplex Red was

148 obtained from Sigma Aldrich and the sensitive Amplex UltraRed was provided by Invitrogen,  
149 ThermoFisher Scientific.

150

151 The artificial urine was prepared using urea, creatinine, sodium chloride, sodium bicarbonate,  
152 calcium chloride, sodium phosphate monobasic, citric acid provide from Sigma Aldrich (Saint  
153 Louis, USA) and ammonium sulphate and sodium sulphate obtained from Fischer Scientific  
154 (Waltham, USA). Arginine, tryptophan, serine, glycine leucine and uric acid were used to test  
155 the selectivity of the assay and were purchased from Sigma Aldrich (Saint Louis, USA). Urine  
156 samples were provided by the La Fe Hospital and Clínico Hospital of Valencia, Spain. Dark 96-  
157 well plates and clear 96-well plates used for fluorescence and absorbance measurements  
158 respectively, were provided by Thermo Scientific (Roskilde, Denmark).

159

## 160 2.2 Instruments

161

162 A Varian Cary Fluorescence Spectrophotometer from Agilent (Santa Clara, USA) was used for  
163 fluorescence measurements and a spectrophotometer synergy HT from Biotek Instruments Ltd  
164 (Winooski, USA) was used for absorbance measurements. Characterization of particles by  
165 FTIR-ATR was carried out with a Cary 630 FTIR-ATR spectrophotometer Agilent Technologies  
166 (Böblingen, Germany). A Nikon EFD-3 microscope was used for the optical and fluorescence  
167 images.

168

169 The incubator used for the synthesis of the fusion protein was the Innova 4300 incubator shaker  
170 from New Brunswick Scientific (Enfield, USA). The centrifuge used was megafuge 10R for  
171 larger volume (flacon tubes) and Biofuge pico for small volume (eppendorf) both from Heraeus  
172 Instruments (Hanau, Germany). The pH values were determined with pH meter 3510 from  
173 Jenway (Staffordshire, UK) calibrated at room temperature with standard buffers.

174

## 175 2.3 Expression and isolation of the protein

176

177 Protein design, expression and isolation has been described previously [33]. The constructs  
178 were designed with a coloured fluorescent protein (mCherry, mCh) to enable easy monitoring of  
179 production, and a silaffin peptide sequence for immobilisation to silica. The plasmid was  
180 designed previously and provided for this project. Before expressing the protein, BL21(DE3) E.  
181 coli containing the desired plasmid were grown overnight in a starter culture of 20 ml Luria  
182 Broth (LB). Then, 200  $\mu$ L from overnight culture was transferred to 20 mL of LB Broth with  
183 kanamycin (10  $\mu$ L, 100 mg/mL) and the solution was left overnight in the 37°C shaking  
184 incubator. The culture was transferred to 200 mL LB Broth with kanamycin (100  $\mu$ L, 100

185 mg/mL) and it was incubated for 3 h in the shaking incubator. Then, isopropyl- $\beta$ -D-1-  
186 thiogalactopyranoside (IPTG) was added as initiator and it was incubated for 4-5 h during  
187 protein expression. Due to the internally fused mCherry label, production could be followed by  
188 the development of the pink colour. The culture was centrifuged at 4300 rpm for 20 min at 4°C.  
189 The supernatant was discarded and the pellet was stored at 4°C. The protein was obtained from  
190 the cell by lysing with lysozyme (10 mg/mL), sonication for 30 s on /30 s off for 3 cycles; 20 s  
191 on / 30 s off for 5 cycles; 10 s / on 10 s off for 10 cycles. The mixture was centrifuged at 13000  
192 rpm for 20 min at 4°C, the supernatant which contained the impure protein was stored at 4°C.

193

#### 194 2.4 Immobilization on silica particles

195

196 The immobilization of R5<sub>2</sub>-mCherry-mSOx-R5-6H on silica particles followed the procedure  
197 reported previously [33] with some modifications. The modified protocol was carried out using  
198 a suspension of silica particles (10 mg/mL, 5 mg in 0.5 mL), prepared in disodium phosphate  
199 buffered saline (100 mM phosphate, 150 mM NaCl, pH 7.5). The mixture was sonicated for 1 h  
200 and then 150  $\mu$ L of crude protein (0.8 mg/mL) was added. The final concentration of the protein  
201 was 0.18 mg/mL. After mixing it by vortex, the suspension was left for 1 h at room temperature  
202 to precipitate. The particles became pink and the supernatant colourless. Finally, it was  
203 centrifuged at 13000 rpm for 5 min. The final protein loading for SiO<sub>2</sub>-R5<sub>2</sub>-mCherry-mSOx-R5-  
204 6H was 24 $\mu$ g protein/mg silica.

205

206 The selectivity of R5<sub>2</sub>-mCherry-mSOx-R5-6H for silica against other materials such as alumina,  
207 titanium oxide, calcium carbonate, cellulose and chitosan and were tested following the same  
208 protocol. Also, the protocol was followed to test the immobilization of R5<sub>2</sub>-mCherry-mSOx-R5-  
209 6H for different particle size of silica.

210

211 To test the R5<sub>2</sub>-mCherry-mSOx-R5-6H loading on silica, different concentration of crude  
212 protein (0.8mg/mL) or pure protein (4mg/mL) were added to 5 mg of silica in 0.5 mL of  
213 disodium phosphate buffer saline (100mM phosphate, 150 mM NaCl pH: 7.4) separately and  
214 the protocol was followed.

215

216 To evaluate the R5<sub>2</sub>-mCherry-mSOx-R5-6H resistance to leaching: the particles were washed  
217 several times with water and buffer and no leaching of the protein from the particles to the  
218 solution was observed. The R5-protein could be partially released in acidic media (pH 4), after  
219 30 min (around 40% of release) while higher release (85%) could be achieved using lysine  
220 solution 1M, pH 7.4.

221

222 For the chemical immobilization of commercially available SOx and HRP, the protocol  
223 followed was developed previously by the Cambridge Analytical Biotechnology group for  
224 protein labelling of silica nanoparticles reported by [36,37]. The modified protocol described  
225 here, the NH<sub>2</sub>-modified silica particles were obtained by mixing TEOS (0.6 mL) in an ammonia  
226 solution (30 % wt, 0.5 mL) and 0.1 g of silica particles. The mixture was stirred for 1 h. then,  
227 APTES (0.2 mL) was added and the mixture was agitated for 4-5 h at room temperature. After  
228 the reaction was completed, the particles were centrifuged, washed several times with water and  
229 ethanol and were dried overnight. Finally, a glutaraldehyde (GA) aqueous solution (1.6 % wt  
230 GA, 1 mL) was added to the obtained GA modified silica particles and the reaction was stirred  
231 for 3 h at room temperature. The particles changed from white to yellow and then, orange. The  
232 GA-silica particles were centrifuged, washed several times with water. Finally, they were  
233 dispersed in a solution of HRP (2 mg/mL, 1mL giving 0.04 HRP/2mg particles) or SOx (1.5  
234 mg/mL) and stirred for 4-5 hours at room temperature. The HRP-SiO<sub>2</sub>Ps and SOx-SiO<sub>2</sub>Ps were  
235 centrifuged and washed three-four times with water and dried overnight.

236

237 Amplex Ultrared was immobilized by mixing TEOS (0.6 mL) in an ammonia solution (30 %  
238 wt, 0.5 mL) and 0.1g of silica particles with stirring for 1 h. 20 µL of stock solution of Amplex  
239 Ultrared in DMSO (10 mg/mL) was then added and stirred for 30 minutes. Finally, the  
240 supernatant was removed by decantation and the particles were dried at room temperature in the  
241 dark for 4 h. The colour of the particles changed from white to pink. The same experimental  
242 process was used for the immobilization of Amplex Red.

243

244 2.5 Estimation of immobilized protein on silica particles

245

246 Protein loading was checked by comparing data from two methods. Taking advantage of the  
247 fluorescence of the fused internal mCherry reference, direct estimation of immobilized protein  
248 is possible. The percentage of immobilized protein was calculated by the difference of  
249 fluorescence intensity ( $\lambda_{ex/em}$  587 / 607 nm) of the free protein in the supernatant at the  
250 beginning ( $I_{sol}$ ) and end ( $I_{sup}$ ) of the immobilisation, in equation (eq.) 1 :

251

$$252 \quad \% \text{ of immobilized protein on silica} = 100 - \left( \frac{I_{sol} - I_{sup}}{I_{sol}} \cdot 100 \right) \quad (\text{eq. 1})$$

253

254 The Bradford assay [38] for the estimation of protein concentration using Coomassie brilliant  
255 blue and bovine serum albumin as a standard was employed.

256

257 2.6 Estimation of the enzyme activity

258

259 Trinder's colorimetric assay was adapted for sarcosine oxidase and used to measure the activity  
260 of R5<sub>2</sub>-mCherry-mSOx-R5-6H in solution and immobilised on SiO<sub>2</sub> particles compared with  
261 commercial sarcosine oxidase. The assay was carried out in disodium phosphate buffer (150-  
262 300  $\mu$ L, 10 mM, pH 7.5) with 4-aminoantipyrine (50  $\mu$ L, 1% w/v), phenol (50  $\mu$ L, 1% w/v),  
263 sarcosine (50  $\mu$ L, 2 M), HRP (50  $\mu$ L, 0.4 mg/mL) and the R5<sub>2</sub>-mCherry-SOx-R5-6H (10  $\mu$ L, 4  
264 mg/mL) or SiO<sub>2</sub>-R5<sub>2</sub>-mCherry-SOx-R5-6H (2.5 mg, 4 mg/mL) or commercial sarcosine oxidase  
265 (10  $\mu$ L, 2.4 mg/mL). After 5 min, 2.5 mL of ethanol was added to stop the reaction and the  
266 absorbance was registered at 480 nm. Total protein was measured by Bradford assay [42].  
267 Specific activity was estimated by calculating the Units of enzyme activity per mg of total  
268 protein measured.

269

270 A similar protocol was used to measure the activity of HPR and HRP-SiO<sub>2</sub> particles. A solution  
271 of disodium phosphate buffer (300  $\mu$ L, 10 mM, pH 7.5) with 4-aminoantipyrine (50  $\mu$ L, 1%  
272 w/v), phenol (50  $\mu$ L, 1% w/v), H<sub>2</sub>O<sub>2</sub> (50  $\mu$ L, 2M) and the HRP (10  $\mu$ L, 0.4 mg/mL) or 2 mg of  
273 HRP-SiO<sub>2</sub>Ps (containing 40 $\mu$ g protein). After 5 min, 2.5 mL of ethanol was added to stop the  
274 reaction and the absorbance was registered at 480 nm.

275

## 276 2.7 Sarcosine measurements

277

278 Preparation of artificial urine. Minimal artificial urine has been constituted for different  
279 purposes [39]. In this case artificial urine was constituted based on the Brooks and Keevil  
280 recipe, adjusted to be protein-free at pH = 6.2 and comprising of urea (170 mM), ammonium  
281 sulphate (12.5 mM), sodium chloride (90 mM), sodium bicarbonate (25 mM), sodium sulfate  
282 (10 mM), creatinine (5.30 mM), calcium chloride (2.5 mM) sodium phosphate monobasic  
283 anhydrous (7 mM), citric acid (2 mM). The solution was stored in the refrigerator (4 °C) until  
284 use.

285

286 Determination of sarcosine using the reagents in solution. The determination of the sarcosine  
287 was based an enzyme linked assay using sarcosine oxidase and the indirect detection of H<sub>2</sub>O<sub>2</sub>,  
288 using Amplex Ultrared (AR) and horseradish peroxidase (HRP) as a catalyst (See Fig. 1B).  
289 Different volumes of sarcosine solution (0-10  $\mu$ L, 100  $\mu$ M) were added to 70  $\mu$ L artificial urine  
290 or urine, followed by 10  $\mu$ L of HRP 0.4 mg/mL and 10  $\mu$ L of SOx 1.2 mg/mL and 10  $\mu$ L of AR  
291 (100  $\mu$ M) to a final volume of 100  $\mu$ L. After reaction for 20 min at room temperature in the  
292 dark, the fluorescence was measured ( $\lambda_{ex/em}$  530 / 582 nm). The increment of fluorescence  
293 intensity of sarcosine standard ( $I_{Sar}$ ) with respect to the blank ( $I_0$ ) was plotted against the



294 concentration of sarcosine and expressed as follows:  $I_{\text{stand}} - I_0 = a + b [\text{Sarcosine}]$

295

296 Determination of sarcosine using the immobilized reagents on silica particles. Different  
297 volumes of sarcosine solution (0-10  $\mu\text{L}$ , 100  $\mu\text{M}$ ) were added to a final volume of 100  $\mu\text{L}$  of  
298 artificial urine containing 5 mg of protein-SiO<sub>2</sub> particles, 2 mg of HRP-SiO<sub>2</sub> particles and 5 mg  
299 of AR-SiO<sub>2</sub> particles. After reaction for 20 min at room temperature in the dark, the  
300 fluorescence was measured ( $\lambda_{\text{ex/em}}$  530 / 582 nm) as above. The same experimental process was  
301 followed in urine to obtain the calibration curve for sarcosine standards in control urine.

302

303 Well-cards were produced a 5mm diameter wells, cut from 1mm PMMA and sealed on one side  
304 with PCR plate seal (Thermo Scientific Adhesive PCR Plate Seal). 4  $\mu\text{L}$  each of HRP (0.4  
305 mg/mL), sarcosine (0-5 $\mu\text{M}$  final concentration) and AR (10 $\mu\text{M}$ ) were added to 125 $\mu\text{g}$  silica-  
306 R5<sub>2</sub>-mCherry-mSOx-R5-6H suspended in artificial urine (20 $\mu\text{L}$  total assay volume).  
307 Fluorescence intensity was recorded with an FFEI reader (505nm LED for excitation and a  
308 CCD RGB linear sensor for detection). Rate of change of average intensity in the well was  
309 plotted against final concentration of sarcosine, blank subtracted.

310

311 The design and construction of the hourglass sensors has been described in detail elsewhere [33]  
312 for the protein modified silica. They were produced by laser cutting the hourglass shape from  
313 2mm PMMA and sealing both sides with PCR plate seal (Thermo Scientific Adhesive PCR  
314 Plate Seal). A suspension (total 220 $\mu\text{L}$ ) of the R5<sub>2</sub>-mCherry-mSOx-R5 immobilized on silica (1  
315 mg silica, 0.025 mg/mL protein per 1mg silica) was mixed with AR (10 $\mu\text{L}$ , 100 $\mu\text{M}$ ), HRP  
316 (10 $\mu\text{L}$ , 0.4mg/mL) and sarcosine (final concentrations 0 $\mu\text{M}$  - 11.75 $\mu\text{M}$ ) in artificial urine  
317 /urine was loaded into the device. The device was inverted twice for mixing, each time  
318 allowing the particles to settle to the bottom (60s). Fluorescence intensity was recorded with an  
319 FFEI reader (505nm LED for excitation and a CCD RGB linear sensor for detection) every  
320 minute for 18min. The images were analysed for grey scale intensity of the red channel in the  
321 detection area using ImageJ software.

322

323 Preliminary analysis of urine samples. Samples from 5 healthy volunteers and 10 cancer  
324 patients were provided from Hospital la Fe and the Clinic Hospital, Valencia, Spain and were  
325 stored at -20°C until testing. The samples were brought to room temperature for 10 min and  
326 used for the assay without treatment or dilution. For the assay, 100  $\mu\text{L}$  of urine containing 5 mg  
327 of protein-SiO<sub>2</sub> particles (containing <120 $\mu\text{g}$  protein), 2 mg of HRP-SiO<sub>2</sub> particles (containing  
328 <40 $\mu\text{g}$  protein) and 5 mg of AR-SiO<sub>2</sub> particles. After reaction for 20 min at room temperature in  
329 the dark, the fluorescence was measured at ( $\lambda_{\text{ex/em}}$  530 / 582 nm). The increment of fluorescence  
330 intensity of sarcosine standard ( $I_{\text{Sar}}$ ) with respect to the blank; real urine with a sarcosine content

331 below LOD, ( $I_0$ ), for each sample was interpolated on the calibration curve of sarcosine  
332 standards in urine in order to obtain concentration of sarcosine.

333

## 334 2.8 Selectivity and stability

335

336 For the selectivity, stock solutions of amino acids such as alanine, arginine, glycine, leucine,  
337 serine and tryptophan and uric acid were prepared at concentration of 1 mM. The solutions were  
338 diluted in artificial urine to final concentrations of 10  $\mu$ M. A mixture of all of them with  
339 sarcosine were prepared to final concentrations of 10  $\mu$ M. In addition, a sarcosine standard of  
340 10  $\mu$ M in artificial urine ( $I_{Sar}$ ) and a blank ( $I_0$ ) was used as a reference. Then, 5 mg of protein-  
341 SiO<sub>2</sub>Ps, 2 mg of HRP-SiO<sub>2</sub>Ps and 5 mg of AR-SiO<sub>2</sub>Ps were added to 100  $\mu$ L of each diluted  
342 solutions ( $I_i$ ) and after reaction for 20 min at room temperature in the dark, the fluorescence was  
343 measured at excitation/ emission wavelength 530 / 582 nm. The relative fluorescence was  
344 calculated as follows:

345

$$346 \text{ Relative fluorescence (\%)} = \frac{I_i - I_0}{I_{Sar} - I_0} \cdot 100 \quad (\text{eq. 2})$$

347

348 For the stability of the mSOx, a solution of commercial SOx (2.4 mg/mL) was stored for 90  
349 days at room temperature. The obtained R5<sub>2</sub>-mCherry-SOx-R5-6H and the immobilized protein  
350 on silica were also stored at room temperature for 90 days. A fresh solution of commercial SOx  
351 at 2.4 mg/mL prepared before the analysis as well as just expressed protein and immobilized on  
352 silica were used as a reference. A volume of 10  $\mu$ L of fresh ( $I_{i 0 \text{ day}}$ ) and stored solutions ( $I_{i 90 \text{ days}}$ )  
353 of the commercial SOx, R5<sub>2</sub>-mCherry-SOx-R5-6H or 5 mg of SiO<sub>2</sub>-R5<sub>2</sub>-mCherry-SOx-R5-6H  
354 were dispersed in artificial urine. Then, 10  $\mu$ L of sarcosine standard (100  $\mu$ M) or 10  $\mu$ L of water  
355 for the blank ( $I_0$ ), 10  $\mu$ L of HRP 0.4 mg/mL and 10  $\mu$ L Amplex Ultrared were added. The final  
356 volume of each one was 100  $\mu$ L. After reaction for 20 min at room temperature in dark, the  
357 fluorescence was measured at excitation/ emission wavelength 530 / 582 nm. The relative  
358 fluorescence was calculated as follows:

359

$$360 \text{ Relative fluorescence (\%)} = \frac{I_{i 0 \text{ day}} - I_0}{I_{i 90 \text{ days}} - I_0} \cdot 100 \quad (\text{eq. 3})$$

361

362 For the stability of the fluorescence of mCherry-6H and R5-mCherry-6H on thin-layer  
363 chromatography (TLC) was measured by deposition of 1 $\mu$ L of each (1mg/mL) on silica TLC  
364 plates using glass capillaries. Then, the plates were left at room temperature for 1 month.  
365 Images of the spot were taken under the fluorescence microscope and fluorescence scans were  
366 performed with an FFEI reader (505nm LED for excitation and a CCD RGB linear sensor for

367 detection) at various time points. Fluorescence intensity in the red channel of the scans was  
368 quantified using ImageJ.

369

370

371

### 372 **3. Results and discussion**

373

#### 374 3.1 Components for a silica-SOx biosensor platform.

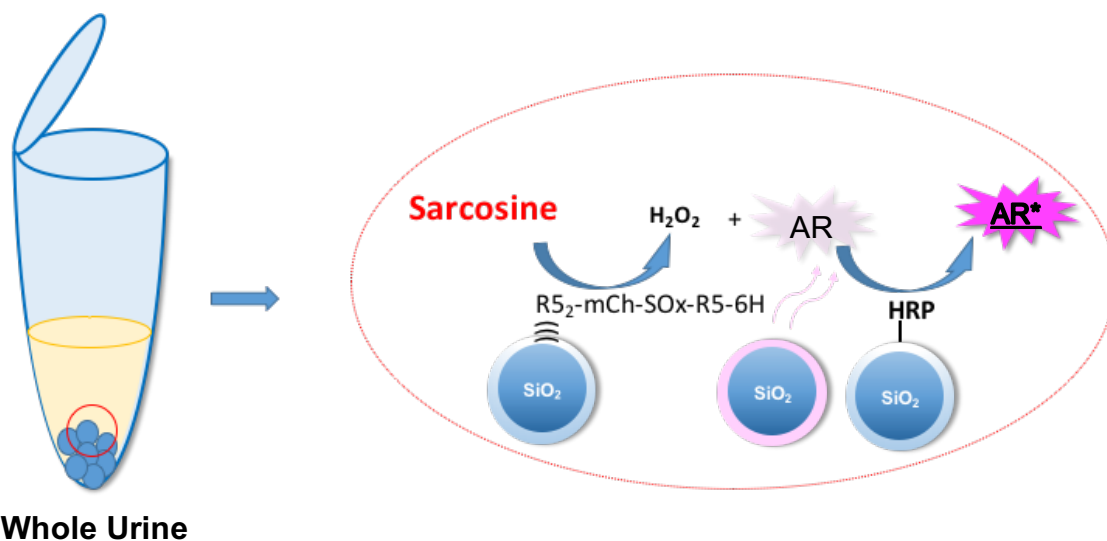
375

376 Sarcosine oxidase belongs to the same family of enzymes as the ubiquitous glucose oxidase, so  
377 that in considering an approach to sarcosine measurement in urine, many lessons can be learned  
378 from the long history of glucose oxidase biosensors. However, in comparison with the two  
379 electron oxidation mechanism involving glucose oxidase [40], which has a specific activity  
380 ranging from 172-300 U/mg ( $\mu\text{mol}/\text{min}/\text{mg}$ ), the specific activity for the one electron process  
381 with sarcosine oxidase is more than an order of magnitude lower. This poses significantly  
382 greater challenges in localizing sufficient enzyme in the vicinity of a transducer to generate a  
383 measurable signal for a biosensor and retaining sufficient activity in the immobilisation process.  
384 Using the classical glutaraldehyde coupling method for protein crosslinking, the specific  
385 activity of sarcosine oxidase (SOx) is reduced from  $\sim 9\text{U}/\text{mg}$  to  $\sim 0.09\text{U}/\text{mg}$ . This can be  
386 improved by chemical coupling with an  $\text{NH}_2$  activated surface on silica particles, but the  
387 residual activity remains too low ( $\sim 0.4\text{U}/\text{mg}$ , table 1) for use in a biosensor. In this work  
388 therefore, we consider self-immobilization directly from the protein without chemical coupling,  
389 by using synthetic biology to design a multicomponent fused protein. The philosophy of this  
390 approach is to include capacity for selective immobilization in the original enzyme design, by  
391 fusing an affinity peptide to the enzyme prior to expression.

392

393 Many affinity peptides have been identified for different materials [31] and in this example we  
394 have considered the use of silica as the core material platform for enzyme presentation. We  
395 have previously expressed a novel fusion protein:  $(\text{R5})_2\text{-mCherry-sarcosine oxidase-R5-6H}$   
396  $(\text{R5}_2\text{-mCherry-SOx-R5-6H})$  [33]. The R5 peptide described here is a 19 amino acid peptide  
397  $(\text{NH}_2\text{-SSKKSGSYSGSKGSKLLIL-COOH})$ . It is derived from diatoms [41, 42] and enables the  
398 protein to “self-immobilise” by adsorption on silica particles (See Fig. 1). It has previously been  
399 reported in protein encapsulation with silica [43] or to enhance precipitation of the protein  
400 through silica encapsulation [44]. In contrast, we do not seek encapsulation, but have selected  
401 this peptide as an affinity tag for immobilisation on silica substrates. Leading on from  
402 preliminary results [33], the application of this silica-immobilised sarcosine oxidase is now  
403 explored in determination of sarcosine together with HRP and Amplex Red as silica bound

404 reagents for a solid state measurement in urine, without the interference that is typical when this  
405 assay is deployed in this sample matrix.



406

407

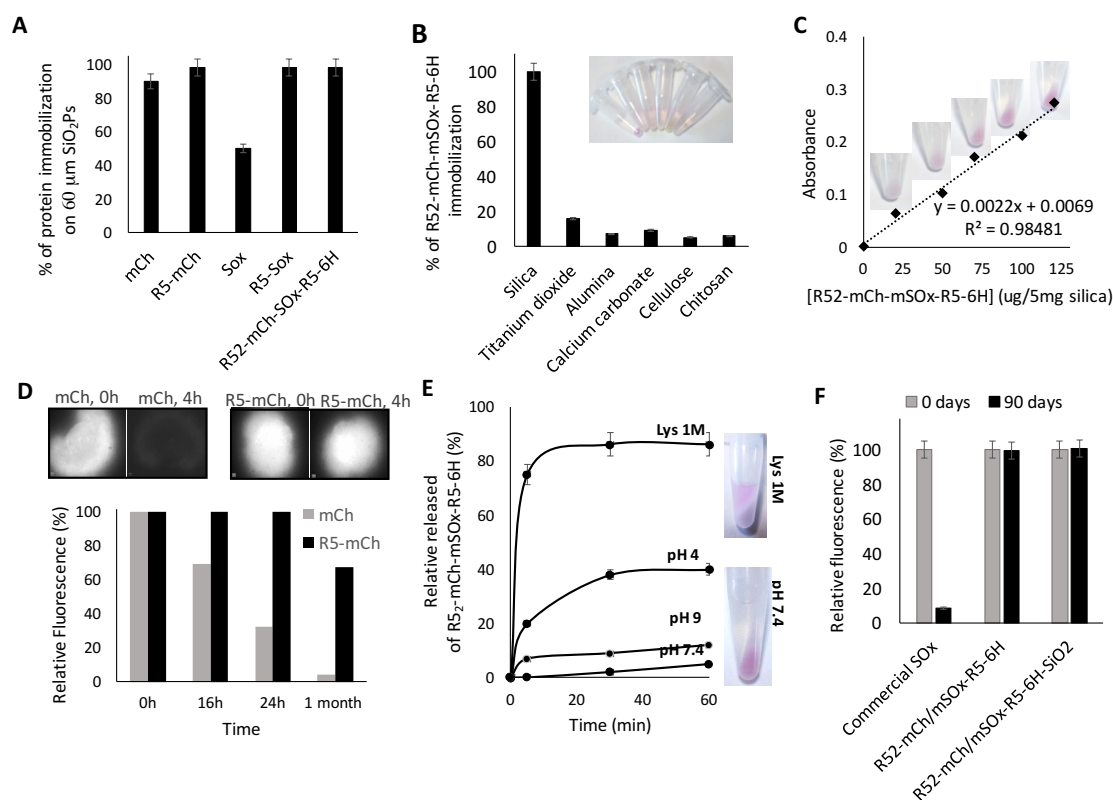
408 **Fig. 1.** Scheme of the biosensor platform for the assay of sarcosine determination in urine. (R5)<sub>2</sub>-  
409 mCherry-Sarcosine oxidase-R5-6H, the catalyst horseradish peroxidase (HRP) and the fluorophore  
410 Amplex Ultrared (AR, pink surface on silica particle) were immobilized on silica particles. The sarcosine  
411 oxidase generates H<sub>2</sub>O<sub>2</sub> in the presence of sarcosine which in turn results in the conversion of AR to a  
412 fluorescent product by HRP.

413

414 A fluorometric assay for sarcosine has been proposed based on the pathway reported in Fig.1.  
415 Central to the design of this system is the role of the R5 peptide on protein immobilization on  
416 silica. The experimental process of R5-protein immobilization is an easy, fast method where no  
417 additional coupling reagents are needed, other than the protein and the silica substrate in buffer.  
418 The mechanism of protein immobilization on silica involves electrostatic interaction with  
419 release of water at physiological pH, driven by the silanol/siloxide groups on the silica surface  
420 and positively charged residues on the R5 polypeptide [45, 46]. The efficiency of target R5 in  
421 enzyme immobilization on silica particles (Section 2.5, eq.1) was studied comparing the amount  
422 of protein immobilized for R5<sub>2</sub>-mCherry-SOx-R5-6H with native SOx and mCherry. The  
423 immobilization of R5<sub>2</sub>-mCherry-SOx-R5-6H on silica particles resulted in approximately 99%  
424 efficiency based on the inbuilt mCherry fluorescence  $\lambda_{\text{ex/em}} = 587 / 607$  nm of supernatant  
425 solution (Section 2.5, eq. 1) as can be seen in Fig. 2A and very selective to silica as a substrate  
426 (Fig. 2B). For solutions of purified R5<sub>2</sub>-mCherry-SOx-R5-6H enzyme, loading on silica was  
427 proportional to the enzyme concentration in the incubation solution (Fig. 2C) with  
428 immobilisation efficiency independent of enzyme concentration (Fig. S1A).

429

430 In the absence of R5, only ~50% of SOx could be adsorbed non-specifically compared with  
 431 ~99% R5-SOx. A higher level of adsorption was found with mCherry-6H (~80% ) without the  
 432 R5 (See Fig. 2A) but with loss of fluorescence (Fig. 2D). Red fluorescent proteins have been  
 433 seen to have a susceptibility to loss of fluorescence, due to loss of secondary structure and  
 434 denaturing on silica [47]. When mCherry-6H and R5-mCherry-6H are adsorbed onto a silica  
 435 thin layer chromatography plate, Fig. 2D, mCherry-6H is adsorbed but the fluorescence is lost  
 436 rapidly at room temperature for the native enzyme. In contrast, R5-mCherry-6H retained full  
 437 fluorescence activity over 24 hrs, decaying only slowly and still retaining >60% of the original  
 438 activity after one month (See Section 2.8). The R5-tagged mSOx is also resistant to leaching at  
 439 normal physiological pH and even at alkaline pH. It could be partially released in acidic media  
 440 (pH 4) after 30 min (around 40% of release). In addition, lysine (Lys) at high concentrations is  
 441 able to competitively displace the R5 from the silica [48]. It can be seen in Fig. 2E that 85% of  
 442 R5<sub>2</sub>-mCherry-SOx-R5-6H was released using lysine at 1M pH 7.4, however these conditions  
 443 are not representative of urine. In urine, loss of R5<sub>2</sub>-mCherry-SOx-R5-6H from the silica was  
 444 less than 4%.  
 445



446  
 447 **Fig. 2.** A) Protein immobilisation on silica dependent on the presence or absence of the R5 silaffin  
 448 polypeptide component for mCherry and SOx constructs (immobilisation from a solution of 0.4 mg/mL  
 449 protein), B) selectivity of R5<sub>2</sub>-mCherry-mSOx-R5-6H for silica compared with other substrates C) R5<sub>2</sub>-  
 450 mCherry-mSOx-R5-6H loading on silica depending of its concentration in the immobilisation incubation,  
 451 D) Microscopy images of 1 $\mu\text{L}$  of mCherry-6H and R5-mCherry-6H (1 mg/mL) on thin-layer

452 chromatography (TLC) plate and the relative red channel fluorescence intensity (%) measured using an  
 453 FFEI reader and analysed with ImageJ; E) R5<sub>2</sub>-mCherry-mSOx-R5-6H leaching under strong conditions  
 454 lysine 1M, compared with different pH; F) Stability of commercial wildtype SOx, R5<sub>2</sub>-mCherry-mSOx-  
 455 R5-6H in solution and the SiO<sub>2</sub>- R5<sub>2</sub>-mCherry-mSOx-R5-6H at room temperature for 90 days.

456

457 The silica used for the immobilization of the reagents can be obtained from natural resources  
 458 such sand and from rice (Fig. S6) or purchased as narrow or broad range sized particles.  
 459 Immobilisation efficiency (eq. 1) is influenced by silica particle size, and a decrease in  
 460 immobilisation efficiency can be observed for larger particles. The best results were obtained  
 461 for silica particles between 0.25 to 60 μm using concentrations of the protein between 0.2-0.4  
 462 mg/L (See Fig. S1B). This is also consistent with other work using the Car9 silica affinity  
 463 peptide [49]. Silica of sand origin or silica particles of 60 μm were selected due to their easy  
 464 precipitation with the protein, during the protein immobilization process, without need of  
 465 centrifugation.

466

467 The effect of immobilisation on the enzyme activities was also highlighted for the wildtype SOx  
 468 and R5<sub>2</sub>-mCherry-mSOx-R5-6H, measured using the Trinder assay (See Section 2.6). Table 1  
 469 compares the specific activity for mSOx in solution and immobilised on silica using either the  
 470 traditional chemical method of crosslinking with glutaraldehyde to an amino activated silica  
 471 (see Section 2.4) or via the R5 affinity peptide. Although the solution of crude lysate containing  
 472 R5<sub>2</sub>-mCherry-mSOx-R5-6H had a relatively low specific activity of 1.33 U/mg, after selective  
 473 immobilisation on to silica of the R5<sub>2</sub>-mCherry-mSOx-R5-6H from the crude extract, this  
 474 increases to 5U/mg, compared with 7.49 U/mg for the isolated purified protein. For  
 475 comparison, the GA-linked SOx drops to 0.4 U/mg protein on silica, compared with 9.6 U/mg  
 476 in solution.

477

478 **Table 1.** Enzymatic activities measured by Trinder's assay.

Enzyme	mSOx	mSOx GA- linked	mSOx GA- linked on silica	R5 <sub>2</sub> -mCherry-mSOx- R5-6H		R5 <sub>2</sub> -mCherry- mSOx-R5-6H on silica (apparent activity)	HRP	HRP GA-linked on silica
				Crude	Pure			
<b>Activity (U/mg)</b>	9.6±0.5	0.09±0.03	0.4±0.2	1.33±0.13	7.49±0.08	5 ± 0.3	323 ± 5	21 ± 1

479

480 The stability of the free and silica immobilised proteins showed clear differences when studied  
 481 at room temperature over time (60 and 90 days) (Fig. 2). It is clear from this figure that the R5-  
 482 mCherry fusions have produced a more robust protein with almost no loss of activity in 90 days,  
 483 whereas the proteins without R5 lose more than 90% of their relative activity. The data for this

484 robust R5<sub>2</sub>-mCherry-SOx-R5-6H provides a good basis for development of a sarcosine  
485 biosensor.

486

### 487 3.2 Towards a sarcosine biosensor using SiO<sub>2</sub>-R5<sub>2</sub>-mCherry-mSOx-R5-6H

488 The enzyme-SiO<sub>2</sub> particle system allows different assay configurations to be considered. The  
489 SiO<sub>2</sub>-R5<sub>2</sub>-mCherry-mSOx-R5-6H enzyme is very suitable for a packed column/bed format. Fig.  
490 S5 shows the microfluidic system developed recently for an immunoassay biosensor [36],  
491 repurposed here for an enzyme assay. In contrast as reported recently elsewhere [33], utilising  
492 the principles of an hour glass and silica obtained from sand (Fig S6), Fig. S7 shows a thin film  
493 hour-glass cell containing R5<sub>2</sub>-mCherry-mSOx-R5-6H protein on silica. This was filled with  
494 artificial urine and then inverted to cause the silica to fall through the sample and precipitate at  
495 the base. Fig. S6 shows that by obtaining the change in the fluorescent intensity profile through  
496 the cell for a given time interval (6 min was selected) a linear relationship with sarcosine  
497 concentration is revealed. More conventionally Fig. 3A shows the calibration curve for  
498 sarcosine with SiO<sub>2</sub>-R5<sub>2</sub>-mCherry-mSOx-R5-6H particles in artificial urine a simple eppendorf.  
499 As can be seen from the plot, there is good linearity across the range of potential clinical interest  
500 for identifying elevated sarcosine levels (>5μM) in patients with prostate cancer.

501

502 However, the assay can also be formulated to work as a spot test with very low volume samples  
503 (eg 20μL, Fig. 3B) with a fluorescence output that can be read visually against an intensity  
504 match card (see Fig. 3B) to provide a simple positive/negative result. A quantitative  
505 measurement can also be obtained in this format with resolution adjusted for either high or low  
506 sarcosine levels. For example, as can be seen in the plot in Fig. 3B, the reader intensity is set to  
507 give a maximum at 3.5 μM (in the normal clinical range) so that measurement reaches signal  
508 saturation at higher concentrations.

509

510 These preliminary results using artificial urine show promise for further construction of the  
511 SiO<sub>2</sub>-R5<sub>2</sub>-mCherry-mSOx-R5-6H biosensor. However, this requires the coimmobilisation of the  
512 HRP and Amplex Red.

513

### 514 3.3 Addition of HRP-SiO<sub>2</sub>

515

516 The stoichiometric coproduct from the SOx catalysed oxidation of sarcosine is H<sub>2</sub>O<sub>2</sub> which acts  
517 as an indirect measurand of sarcosine, producing a colorimetric product catalysed by HRP (Fig.  
518 1B). However, although horseradish peroxidase (HRP) is widely used in such combinations,  
519 recombinant HRP is difficult to express and has a tendency to form inclusion bodies (IBs) in  
520 E.coli with low yield [50] of active protein. Thus, commercially available peroxidases are

521 largely from plant extracts and are a mixture of acidic and basic isoenzymes. We have  
522 previously shown that some engineered type C R5-HRP isoenzymes, expressed in E.coli can be  
523 produced without IBs, but this isoenzyme has an activity of  $\sim 0.2$ U/mg compared with  
524  $>300$ U/mg for the commercial mixed isoenzyme HRP of plant origin. In this instance, the wild  
525 type mixed acidic and basic HRP isoenzyme with high initial activity, is thus the preferred  
526 enzyme source for a first step in a peroxide linked sarcosine assay. This required a classical  
527 chemical immobilisation of HRP using GA coupling. This does not share the same benefits as  
528 the easy R5 protein modification, of being coupling-reagent free and single step, but provides a  
529 compatible stepwise model for taking the silica platform forward to explore whether sarcosine  
530 can be detected in urine.

531

532 In the HRP-silica containing samples, the FTIR (Fig. S2A) is dominated by a band at  $1089\text{ cm}^{-1}$   
533 which corresponds to Si-O-Si antisymmetric stretching vibrations. The presence of HRP is  
534 indicated by the characteristic absorptions at  $1640$  and  $1540\text{ cm}^{-1}$ , attributed to -CONH- (amide  
535 I) and amide II, respectively (see insert in Fig. S2A). The HRP-SiO<sub>2</sub> particles are green and red  
536 autofluorescent (Fig. S2B) similar to observations in previous reports after glutaraldehyde  
537 crosslinking of serum albumins [51]. These authors attributed this observation to  $\pi$ - $\pi^*$   
538 transitions of the C=O bond and n- $\pi^*$  transition of C=N bond as a result of the  $\alpha,\beta$  unsaturated  
539 aldehyde.

540

541 The activity of HRP-SiO<sub>2</sub> particles (Section 2.6) compared with the free enzyme, showed the  
542 expected loss of activity following glutaraldehyde crosslinking ( $21 \pm 1$  U/mg) (See Table 1)  
543 which is consistent with other reports of reduced activity following glutaraldehyde crosslinking  
544 [52] but nevertheless retains HRP activity at a higher level than the SOx, so that it should not  
545 limit the assay pathway. The SiO<sub>2</sub>-R5<sub>2</sub>-mCherry-SOx-R5-6H and HRP-SiO<sub>2</sub> can thus be  
546 combined for the determination of sarcosine and tested in artificial urine. As can be seen in Fig.  
547 3C, the behaviour observed for the free HRP and HRP-SiO<sub>2</sub> in combination with SiO<sub>2</sub>-R5<sub>2</sub>-  
548 mCherry-SOx-R5-6H was broadly equivalent. This provides a good basis for a fully  
549 immobilised SiO<sub>2</sub>-enzyme system.

550

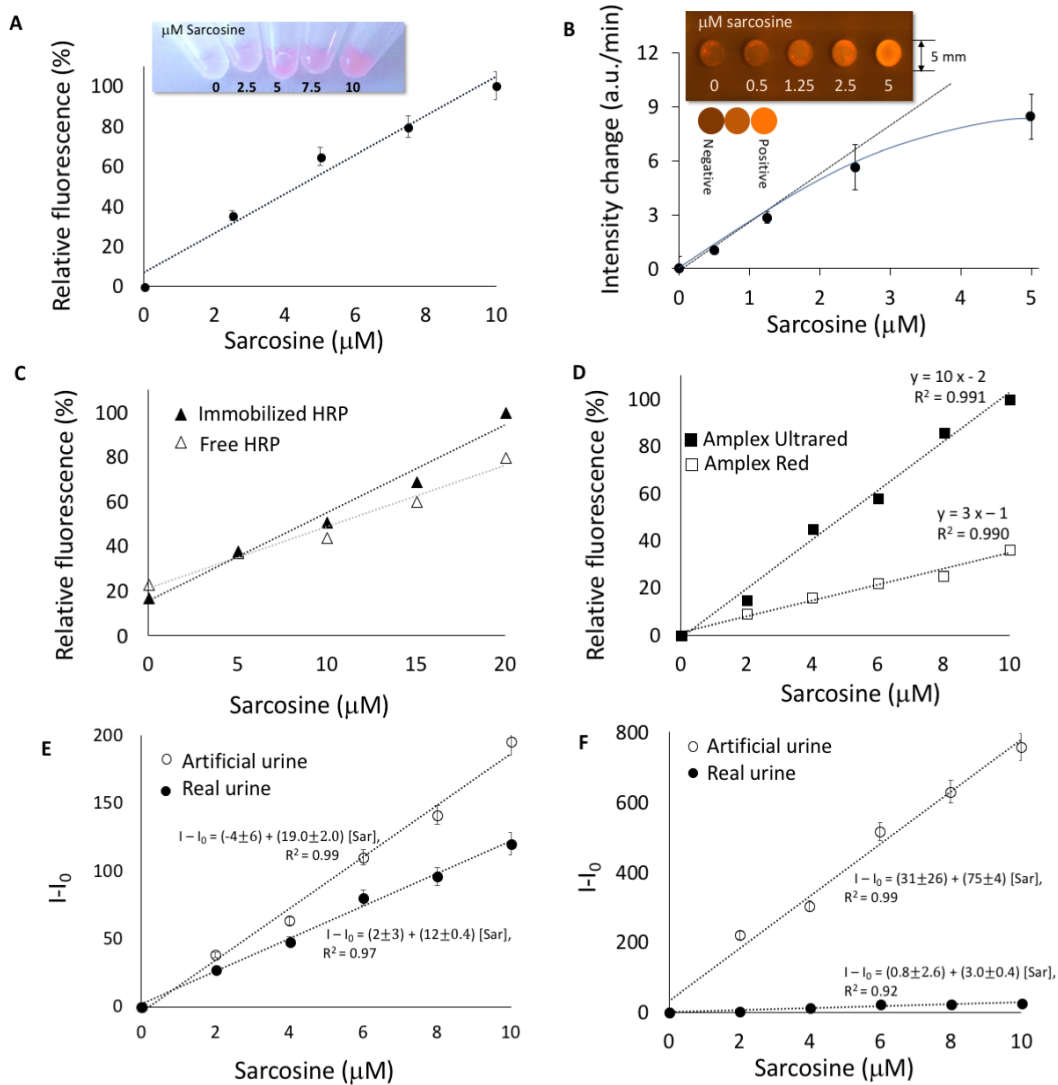
### 551 3.4 Addition of Amplex UltraRed-SiO<sub>2</sub>

552

553 The silica particulate format offers versatility for the assay, so to complete the presentation on  
554 silica, the Amplex Red group of dyes were encapsulated on the surface of silica particles within  
555 a sol-gel using TEOS in basic conditions. The dye-SiO<sub>2</sub> provided a vehicle for quick release and  
556 delivery of the reagent in contact with aqueous solution where the determination of sarcosine  
557 takes place. Under optimised conditions, with HRP-SiO<sub>2</sub> and dye-SiO<sub>2</sub> in sarcosine-spiked real



558 urine, the results showed that Amplex Ultrared (AR) has around 2-fold higher sensitivity than  
 559 Amplex Red (Fig. 3D) in the range of 0-10  $\mu\text{M}$  of sarcosine.  
 560



561

562

563 **Fig. 3.** Calibration curves for sarcosine determination in artificial urine using R5<sub>2</sub>-mCherry-SO<sub>x</sub>-R5-6H-  
 564 SiO<sub>2</sub> together with A), HRP and AR (100 $\mu\text{L}$  sample in eppendorfs); B) HRP and AR in a well-card  
 565 showing a quantitative plot of fluorescence intensity. Visual fluorescent intensity image of well-card for  
 566 20 $\mu\text{L}$  samples shown with qualitative intensity image scale; C) AR and comparing the results with HRP  
 567 and HRP-SiO<sub>2</sub>; D) HRP-SiO<sub>2</sub> and comparing the sensitivity of Amplex Ultrared, AR (in black) against  
 568 Amplex Red (in white) immobilized on silica E) HRP-SiO<sub>2</sub> and AR-SiO<sub>2</sub> compared with F) the  
 569 commercial reagents SO<sub>x</sub>, HRP and AR in solution (note the different y axis scales). E and F tested in  
 570 artificial urine and real urine from a control volunteer. Relative fluorescence measured at  $\lambda_{\text{ex/em}}$  530 / 582  
 571 experimental details in Section 2.7

572

573 3.5 Integrated sarcosine assay in urine

574 The pH of normal urine is within the range of 5.5 to 7 with an average of 6.2 [54] while urine  
575 from cancer patients can be more acidic (pH 5). Amplex Ultrared has a broader useful pH range  
576 from pH5 to 8 compared with Amplex Red from pH 6 to 7 (See Fig. S3B). This shows that the  
577 pH should not affect the Amplex Ultrared for sarcosine determination in samples from either  
578 negative controls or positive patients.

579

580 As mentioned earlier, the normal sarcosine test kit employing SOx suffers from interference for  
581 measurements in urine, producing artificially low results (assay kits warn against use in urine,  
582 but favour measurement in blood or serum, where sarcosine levels are not indicative for  
583 prostatic carcinoma). This problem is also demonstrated here (Fig. 3F) using the commercially  
584 available reagents in solution, where the urine sample, spiked with sarcosine produces a very  
585 low fluorescence at 582nm, that is hardly sensitive to sarcosine concentration and only 4% of  
586 the slope for artificial urine. This suggests that there is an inhibitor of the SOx or other matrix  
587 effect for the reaction in the real urine. In contrast, the fluorescence intensity of the solutions at  
588 582 nm for the silica-bound reagents showed a good linear relationship with sarcosine  
589 concentration between 0 to 10  $\mu$ M, with a slope in urine that is 63 % of that obtained in artificial  
590 urine. It is evident that the silica-immobilised enzyme construct with SOx is less affected by the  
591 urine. By calibration in spiked screened urine from a healthy patient, the system adjusts for this  
592 background and provides excellent sensitivity in the required range, in contrast to the  
593 commercial SOx kit.

594

595 It is known that the urinary amino acid alanine which is at higher concentration than sarcosine  
596 in urine, is an interfering compound in sarcosine analysis by GC or LC coupled mass  
597 spectrometry, due to their equivalent parent and fragment [53-55]. On the other hand, glycine,  
598 which is a product of oxidative demethylation of sarcosine has also been shown to be a substrate  
599 for SOx with low activity. Fig. S3A shows that alanine and glycine as well as some other  
600 amino acids produced only a small fluorescent signal in the absence of sarcosine, as does uric  
601 acid so that, alanine in particular, does not have the same significance as seen with coupled  
602 mass spectrometry detection. Tyrosine and leucine appear to give a 'negative' signal, which  
603 can be correlated with the direct interaction with the Amplex dye, reducing the background  
604 fluorescence. Tyrosine dimerisation with H<sub>2</sub>O<sub>2</sub> in the presence of HRP also forms a fluorescent  
605 product[56], which can influence the final signal, although this effect is typically small at this  
606 wavelength, since the emission is at a lower wavelength. These matrix effects are independent  
607 of SOx concentration and can be accommodated in the background calibration with a combined  
608 effect reducing the overall signal by ~20% on silica, but still retaining the required resolution  
609 for sarcosine determination in clinical sample. In contrast, >80% reduction of the signal is

610 observed with the wildtype SOx in solution and the sarcosine test kits.

611

612

### 613 3.5 Application to urine from prostate cancer patients

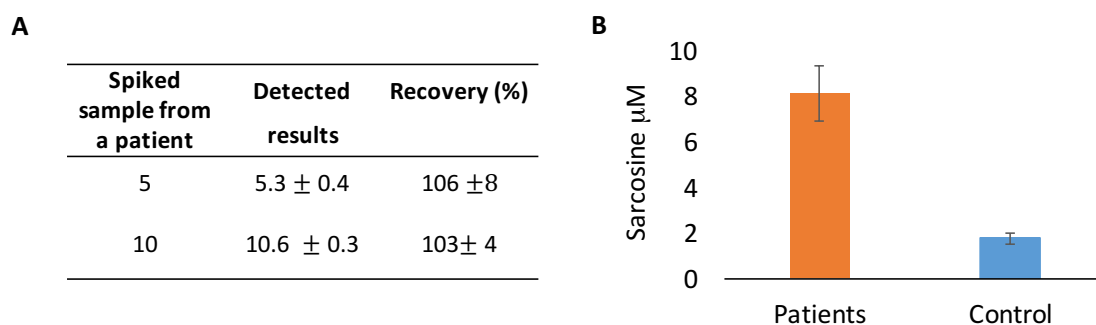
614

615 The validity of the sarcosine sensor to discriminate between samples from healthy volunteers  
616 and prostate cancer patients was tested. The samples were processed without any pre-treatment  
617 and without dilution avoiding sample contamination and reducing the time of the assay. As  
618 mentioned before, the calibration slope obtained for artificial urine and urine was different, due  
619 to a matrix effect. In order to accommodate the matrix, the calibration curve was carried out in a  
620 real urine sample with a sarcosine content below the LOD. To evaluate the accuracy of the  
621 procedure, urine samples from cancer patients were also spiked with 5 and 10  $\mu\text{M}$  of sarcosine.  
622 The recoveries obtained were near to 100% as can be seen in Fig. 4A suggesting that the  
623 calibration was robust. Three replicates were done in all the cases.

624

625 Five samples from healthy volunteers or controls were compared with 10 samples of prostate  
626 cancer patients using the proposed 'silica-enzyme' biosensor. Higher intensities were found for  
627 prostate cancer patients compared with the control (See Fig S4). The concentrations of sarcosine  
628 calculated were 0 to 2.2  $\mu\text{M}$  and 6.8 to 10.6  $\mu\text{M}$  from healthy and patient samples, respectively.  
629 In Fig. 4B, the sarcosine concentration of cancer patients is shown to be about 4 times higher  
630 than for healthy donors. As a first approach, the sensor demonstrated here appears to be able to  
631 discriminate between healthy and prostate cancer patients.

632



633

634 **Fig. 4.** A) The results obtained for a spiked sample from a patient with 5 and 10  $\mu\text{M}$  of sarcosine  
635 ( $n=3$ ). B) Comparison the mean concentrations of sarcosine estimated from urine samples of healthy  
636 volunteers (controls,  $n = 5$ ) and PCa patients (patients,  $n = 10$ ). For more experimental details see Section  
637 2.7.

638

639

640

641 **4. Conclusions**

642

643 A novel fused protein R5<sub>2</sub>-mCherry-Sarcosine oxidase-R5-6H was constructed which has the  
644 ability to self-immobilize on silica particles. The mCherry in the fused protein provided a useful  
645 visual reference throughout the production, isolation and immobilisation of the R5<sub>2</sub>-mCherry-  
646 SOx-R5-6H. This protein showed higher stability than the commercial SOx, and the protein  
647 remained stable for at least 3 months. In addition, it can be calibrated in and remains sensitive in  
648 complex matrices such as urine, while the classical SOx assay suffers from interferences and  
649 loses sensitivity. R5<sub>2</sub>-mCherry-SOx-R5-6H, HRP and Amplex UltraRed were all successfully  
650 immobilized on silica particles to develop a particle based solid state sensor for sarcosine  
651 determination in urine. No sample preparation or treatment was needed and the reaction took  
652 place in urine at room temperature in 10-20 min. The proposed sensor is sensitive in the  
653 required clinical range for sarcosine detection in urine. Furthermore, in this preliminary study, it  
654 was able to discriminate between urine from healthy and prostate cancer patients.

655

656 **Acknowledgements**

657 This research gained support in part under the BBSRC/EPSRC funded Grant No.  
658 BB/L014130/1 and is associated with the synthetic biology SRI <http://www.synbio.cam.ac.uk>.  
659 Members of Cambridge Analytical Biotechnology are acknowledged for their previous work on  
660 protein constructs that provided a library for this work. The new enzymes are available, subject  
661 to material transfer agreements. The Gates Cambridge Trust is acknowledged for scholarship to  
662 CJH. NJ expresses her gratitude to Generalitat Valenciana and European commission for its  
663 postdoctoral grant (APOSTD/113/2016). NJ and PC are grateful to Generalitat Valenciana  
664 (PROMETEO 2016/109) for the financial support received.

665

666

667 **References**

668

- 669 [1] A. John, C.P. Price, Existing and emerging technologies for point-of-care testing, *Clin*  
670 *Biochem. Rev.* 35 (2014) 155-167.
- 671
- 672 [2] S. A. Soper, K. Brown, A. Ellington, B. Frazier, G. Garcia-Manero, V. Gau, S.I. Gutman,  
673 D.F. Hayes, B. Korte, J.L. Landers, D. Larson, F. Ligler, A. Majumdar, M. Mascini, D. Nolte,  
674 Z. Rosenzweig, J. Wang, D. Wilson, Point-of-care biosensor systems for cancer  
675 diagnostics/prognostics, *Biosens. Bioelectron.* 21 (2006) 1932-1942.
- 676 [3] M.A Cuzick, G. Thorat, O.W. Andriole, P.H Brawley, Z. Brown, R.A Culig, L. G. Eeles, F.  
677 C. Ford, L. Hamdy, D. Holmberg, T. J. Ilic, M.D. Key, C.L. Vecchia, M. Hans Lilja Marberger,  
678 F.VL. Meyskens, L.M. Minasian, C. Parker, H.L. Parnes, Sven. Prevention and early detection  
679 of prostate cancer. *Lancet Oncol.* 15 (2014) e484-e492.

680 [4] G.P Haas, N. Delongchamps, O.W. Brawley, C.Y. Wang, G. Roza, The worldwide  
681 epidemiology of prostate cancer: perspectives from autopsy studies. *Can. J. Urol.* 15 (2008)  
682 3866-3871.

683 [5] M. Rigau, J. Morote, M.C. Mir, C. Ballesteros, I. Ortega, A. Sanchez, E. Colás, M. Garcia,  
684 A. Ruiz, M. Abal, J. Planas, J. Reventós, A. Doll, PSGR and PCA3 as biomarkers for the  
685 detection of prostate cancer in urine. *Prostate.* 70 (2010) 1760-1767.

686 [6] E.D. Crawford, K.O Rove, E.J. Trabulsi, J. Qian, K.P. Drewnowska, J.C. Kaminetsky, T.K.  
687 Huisman, M.L. Bilowus, S.J. Freedman, W.L. Glover, D.G. Bostwick, Diagnostic performance  
688 of PCA3 to detect prostate cancer in men with increased prostate specific antigen. *J. Urol.* 188,  
689 (2010) 1726-1731.

690 [7] D.L. Cao, D.W. Ye, H.L. Zhang, Y. Zhu, Y.X. Wang, X.D. Yao. A multiplex model of  
691 combining gene-based, protein-based, and metabolite-based with positive and negative markers  
692 in urine for the early diagnosis of prostate cancer. *Prostate.* 71 (2010) 700-710.

693 [8] S. Sharma, J. Zapatero-Rodríguez, R. O'Kennedy. Prostate cancer diagnostics: Clinical  
694 challenges and the ongoing need for disruptive and effective diagnostic tools. *Biotechnol. Adv.*  
695 35 (2017) 135-149.

696 [9] J. Lattanzi, S. McNeely, A. Hanlon, I. Das, T.E. Schultheiss, G.E. Hanks, Daily CT  
697 localization for correcting portal errors in the treatment of prostate cancer. *Int. J. Radiat. Oncol.*  
698 *Biol. Phys.* 41 (1998) 1079-1086.

699 [10] C.J Harvey, J. Pilcher, I. Richenberg, U. Patel, F. Frauscher, Applications of transrectal  
700 ultrasound in prostate cancer. *BIR.* 85 (2012) S3–S17.

701 [11] H.A. Van Vugt, M.J. Roobol, M. Busstra, P. Kil, E.H. Oomens, I.J. de Jong, C.H. Bangma,  
702 E.W. Steyerberg, I. Korfage, Compliance with biopsy recommendations of a prostate cancer  
703 risk calculator. *BJU Int.* 109 (2012) 1480-1488.

704 [12] H. Schoder, S.M. Larson, Positron emission tomography for prostate, bladder, and renal  
705 cancer. *Semin. Nucl. Med.* 34 (2004) 274-292.

706 [13] M.S. Khan, K. Dighe, Z. Wang, I. Srivastava, E. Daza, A.S. Schwartz-Dual, J. Ghannam,  
707 S.K. Misra, D. Pan. Detection of prostate specific antigen (PSA) in human saliva using an ultra-  
708 sensitive nanocomposite of graphene nanoplatelets with diblock-co-polymers and Au  
709 electrodes. *Analyst* 143 (2018) 1094-1103.

710 [14] J.S. Myers, A.K. von Lersner, C.J. Robbins, Q.X.A. Sang, Differentially Expressed Genes  
711 and Signature Pathways of Human Prostate Cancer. *PLoS One.* 10, 2015, e0145322

712 [15] A.J. Armstrong, M.A Eisenberger, S. Halabi, S. Oudard, D.M. Nanus, D.P. Petrylak, A.O.  
713 Sartor, H.I. Scher, Biomarkers in the management and treatment of men with metastatic  
714 castration-resistant prostate cancer. *Eur. Urol.* 61 (2011) 549-559.

715 [16] A. Sreekumar, M.L. Poisson, T.M. Rajendiran, A.P. Khan, Q. Cao, J.D. Yu, B. Laxman, R.  
716 Mehra, R.J. Lonigro, Y. Li, M.K. Nyati, A. Ahsan, S. Kalyana-Sundaram, B. Han, X. Cao, J.

717 Byun, G.S. Omenn, D. Ghosh, S. Pennathur, D.C. Alexander, A. Berger, J.R. Shuster, J.T. Wei,  
718 S. Varambally, C. Beecher, A.M. Chinnaiyan, Metabolomic profiles delineate potential role for  
719 sarcosine in prostate cancer progression. *Nature*. 457 (2009) 910–914.

720 [17] D. Pacik, M. Plevova, L. Urbanova, Z. Lackova, V. Strmiska, A. Necas, Z. Heger, V.  
721 Adam, Identification of Sarcosine as a Target Molecule for the Canine Olfactory Detection of  
722 Prostate Carcinoma *Sci. Rep.* 8 (2018) 4958.

723 [18] N. Cernei, Z. Heger, J. Gumulec, Z. Ondrej, M. Masarik, P. Babula, Sarcosine as a  
724 Potential Prostate Cancer Biomarker—A Review. *Int. J. Mol. Sci.* 14 (2013) 13893-13908.

725 [19] A.P. Khan, T.M. Rajendiran, B. Ateeq, I.A. Asangani, J.N. Athanikar, A.K. Yocum, R.  
726 Mehra, J. Siddiqui, G. Palapattu, J.T. Wei, G. Michailidis, A. Sreekumar, A.M. Chinnaiyan,  
727 The role of sarcosine metabolism in prostate cancer progression. *Neoplasia* 15 (2013) 491–501.

728 [20] Z. Heger, M.A. Rodrigo, P. Michalek, H. Polanska, M. Masarik, V. Vit, M. Plevova, D.  
729 Pacik, T. Eckschlager, M. Stiborova, V. Adam. Sarcosine Up-Regulates Expression of Genes  
730 Involved in Cell Cycle Progression of Metastatic Models of Prostate Cancer. *PLoS One*. 8 11  
731 (2016) e0165830.

732 [21] M.A.M Rodrigo, V. Strmiska, E. Horackova, H. Buchtelova, V. Adam, P. Michalek, M.  
733 Stiborova, T. Eckschlager, Z. Heger, Sarcosine influences apoptosis and growth of prostate cells  
734 via cell-type specific regulation of distinct sets of genes. *The Prostate*. 78, (2018) 104–112.

735 [22] Y.Q. Jiang, X.L. Cheng, C.A. Wang, Y.F. Ma. Quantitative determination of sarcosine and  
736 related compounds in urinary samples by liquid chromatography with tandem mass  
737 spectrometry. *Anal. Chem.* 82 (2010) 9022–9027.

738 [23] E. Biavardi, C. Tudisco, F. Maffei, A. Motta, C. Massera, G.G. Condorelli, E. Dalcanale,  
739 Exclusive recognition of sarcosine in water and urine by a cavitand-functionalized silicon  
740 surface. *Proc. Natl. Acad. Sci. USA*. 109 (2012) 2263-2268.

741 [24] G. Valenti, E. Rampazzo, E. Biavardi, E. Villani, G. Fracasso, M. Marcaccio, F. Bertani,  
742 D. Ramarli, E. Dalcanale, F. Paoluccia, L. Prodi. An electrochemiluminescence-supramolecular  
743 approach to sarcosine detection for early diagnosis of prostate cancer. *Faraday Discuss.* 185  
744 (2015) 299-309.

745 [25] Z. Heger, N. Cernei, S. Krizkova, M. Masarik, P. Kopel, P. Hodek, O. Zitka, V. Adam, R.  
746 Kizek, Paramagnetic nanoparticles as a platform for FRET-based sarcosine picomolar detection.  
747 *Sci. Rep.* 5 (2015) 8868.

748 [26] T.S. Rebelo, C.M. Pereira, M.G. Sales, J.P. Noronha, J. Costa-Rodrigues, F. Silva, M.H.  
749 Fernandes, Sarcosine oxidase composite screen-printed electrode for sarcosine determination in  
750 biological samples. *Anal. Chim. Acta.* 850 (2014) 26-32.

751 [27] J.M. Lan, W. Xu, Q. Wan, X. Zhang, J. Lin, J. Chen, J. Chen. Colorimetric determination  
752 of sarcosine in urine samples of prostatic carcinoma by mimic enzyme palladium nanoparticles.  
753 *Anal. Chim. Acta.* 825 (2014) 63–68.

754 [28] C. Burton, S. Gamagedara Y.F. Ma. A novel enzymatic technique for determination of  
755 sarcosine in urine samples. *Anal. Methods*. 4 (2012) 141–146.

756 [29] C. Garcia-Galan, A. Berenguer-Murcia, R. Fernandez-Lafuente, R.C. Rodrigues, Potential  
757 of different enzyme immobilization strategies to improve enzyme performance. *Adv. Synth.*  
758 *Catal.* 353 (2011) 2885–2904.

759 [30] U. Guzik, Hupert-Kocurek K, D Wojcieszynska. Immobilization as a Strategy for  
760 Improving Enzyme Properties-Application to Oxidoreductases. *Molecules* 19 (2014) 8995–  
761 9018.

762 [31] E.A.H. Hall, S. Chen, J. Chun, Y. Du, Z. Zhao. A molecular biology approach to protein  
763 coupling at a biosensor interface. *Trends Analyt. Chem.* 79 (2016) 247-256.

764 [32] J. Peccoud, Synthetic biology: fostering the cyber-biological revolution. *Synth. Biol.* 1  
765 (2016) 1-7.

766 [33] C.J. Henderson, E. Pumford, R. Daly, E.A.H. Hall, *Biomaterials* 193 (2019) 58-70.

767 [34] V. Puddu, C.C. Perry, Peptide adsorption on silica nanoparticles: evidence of hydrophobic  
768 interactions. *ACS Nano.* 6 (2012) 6356–6363.

769 [35] S. Datta, L.R. Christena, Y.R.S. Rajaram, Enzyme Immobilization: An Overview on  
770 Techniques and Support Materials. *Biotech* 3 (2013) 1–9.

771 [36] J.F. Engels, C.J. Henderson, R. Daly, R. Renneberg, E.A.H. Hall. A lateral flow channel  
772 immunoassay combining a particle binding zone geometry with nanoparticle labelling  
773 amplification. *Sens. Actuators, B-Chem.* 262 (2018) 1-8.

774 [37] Q. Chang, H. Tang. Immobilization of Horseradish Peroxidase on NH<sub>2</sub>-Modified Magnetic  
775 Fe<sub>3</sub>O<sub>4</sub>/SiO<sub>2</sub> Particles and Its Application in Removal of 2,4-Dichlorophenol. *Molecules* 19  
776 (2014) 15768-15782.

777 [38] M. Bradford, A rapid and sensitive method for the quantitation of microgram quantities of  
778 protein utilizing the principle of protein-dye binding. *Anal. Biochem.* 72 (1976) 248-254.

779 [39] T. Brooks, C.W. Keevil. A simple artificial urine for the growth of urinary pathogens. *Lett*  
780 *Appl Microbiol.* 24 (1997) 203-206.

781 [40] T. Tsuge, O. Natsuaki, K. Ohashi, Purification, properties, and molecular features of  
782 glucose oxidase from *Aspergillus niger*. *J. Biochem.* 79 (1975) 835–43.

783 [41] C.C. Lechner, C.F.W. Becker, Modified silaffin R5 peptides enable encapsulation and  
784 release of cargo molecules from biomimetic silica particles. *Bioorg. Med. Chem.* 21 (2013)  
785 3533–3541.

786 [42] C.C Lechner, C.F.W. Becker, Silaffins in Silica Biomineralization and Biomimetic Silica  
787 Precipitation. *Mar Drugs* 13 (2015) 5298-5333.

788 [43] O. Choi, B.C. Kim, J.H. An, K. Min. Y.H. Kim, Y. Um, M.K. Oh, B.I. Sang, A biosensor  
789 based on the self-entrapment of glucose oxidase within biomimetic silica nanoparticles induced  
790 by a fusion enzyme. *Enzyme Microb. Technol.* 49 (2011) 441–445.

791 [44] D.H. Nam, J.O. Lee, B.I. Sang, K. Won, Y.H. Kim, Silaffin peptides as a novel signal  
792 enhancer for gravimetric biosensors. *Appl. Biochem. Biotechnol.* 170 (2013) 25–31.

793 [45] S.K. Parida, S. Dash, S. Patel, B.K. Mishra, Adsorption of organic molecules on silica  
794 surface. *Adv. Colloid. Interface. Sci.* 121 (2006) 77–110.

795 [46] A.A. Vertegel, R.W. Siegel, S.J. Dordick, Silica nanoparticle size influences the structure  
796 and enzymatic activity of adsorbed lysozyme. *Langmuir* 20 (2004) 6800–6807.

797 [50] Gundinger, T., Spadiut, O., 2017. *J. Biotechnol.* 248, 15–24.

798 [47] M. Soumbo, A. Pugliara, M.-C. Monje, C. Roques, B. Despax, C. Bonafos, R. Carles, A.  
799 Mlayah, K. Makasheva, Physico-Chemical Characterization of the Interaction of Red  
800 Fluorescent Protein-DsRed With Thin Silica Layers. *IEEE. Trans. Nanobioscience*, 15 (2016)  
801 412–417.

802 [48] W. Yang, B. Hellner, F. Baneyx, Self-Immobilization of Car9 Fusion Proteins within High  
803 Surface Area Silica Sol–Gels and Dynamic Control of Protein Release. *Bioconjugate Chem.* 27  
804 (2016) 2450–2459.

805 [49] J. Soto-Rodríguez, B.L. Coyle, A. Samuelson, K. Aravagiri, F. Baneyx, Affinity  
806 purification of Car9-tagged proteins on silica matrices: Optimization of a rapid and inexpensive  
807 protein purification technology. *Protein Expression and Purification*, 135 (2017) 70-77.

808 [51] X. Ma, D. Hargrove, Q. Dong, D. Song, J. Chen, S. Wang, X. Lu, Y.K. Cho, T.-H. Fan,  
809 Yu, Lei. Novel green and red autofluorescent protein nanoparticles for cell imaging and in vivo  
810 biodegradation imaging and modelling. *RSC Advanc*, 6 (2016) 50091-50099.

811 [52] H. Ashraf, Q. Husain, Stabilization of DEAE cellulose adsorbed and glutaraldehyde  
812 crosslinked radish (*Raphanus sativus*) peroxidase. *JSIR* (2010) 613-620.

813 [53] C. Burton, S. Gamagedara, Y. Ma, Partial enzymatic elimination and quantification of  
814 sarcosine from alanine using liquid chromatography-tandem mass spectrometry. *Anal. Bioanal.*  
815 *Chem.* 405 (2013) 3153–3158.

816 [54] F. Jentzmik, C. Stephan, K. Miller, M. Schrader, A. Erberdobler, G. Kristiansen, M. Lein, K.  
817 Jung. Sarcosine in Urine after Digital Rectal Examination Fails as a Marker in Prostate Cancer  
818 Detection and Identification of Aggressive Tumours. *Eur Urol.* 58 (2010) 12–18

819 [55] C. Rose, A. Parker, B. Jefferson, E. Cartmell, The Characterization of Feces and Urine: A  
820 Review of the Literature to Inform Advanced Treatment Technology. *Crit. Rev. Environ. Sci.*  
821 *Technol.* 45 (2015) 1827–1879.

822 [56] M Zhang, Q Lv, N Yue, H Wang Study of fluorescence quenching mechanism between  
823 quercetin and tyrosine-H<sub>2</sub>O<sub>2</sub>-enzyme catalyzed product *Spectrochimica Acta Part A: Molecular*  
824 *and Biomolecular Spectroscopy* 72, (2009), 572-576

825

826



